Supplementary Information

Modular assembly of soft deployable structures and robots

*Wei Wang, Nam-Geuk Kim, Hugo Rodrigue, and Sung-Hoon Ahn**

Preparation of Materials. SMA wires (55wt% Ni, 45wt% Ti, Flexinol) with a diameter of 0.203 mm are used as the smart material, a thin polyvinyl chloride (PVC) plate with a thickness of 0.3 mm as the flexible reinforcement. Polydimethylsiloxane (PDMS) (Sylgard 184, Dow Corning) is used as the polymeric matrix of all actuators and acrylonitrile butadiene styrene (ABS) is used for the embedded stiff reinforcement and mold of all actuators with the ABS parts being manufacturing by fused deposition modeling (FDM) machine (Dimension 768 SST, Stratasys). Circle neodymium (NIB) magnets with a diameter of 10 mm and a thickness of 2 mm as the connectors and NIB magnets were selected due to having the highest romance per unit mass among all commercially available permanent magnets to maximize the strength of the connection while minimizing the mass of the assembled structures. All materials used are commercially available. The main properties of SMA and PDMS are shown in Table S1 and S2.

Fabrication of soft deployable module. The fabrication of soft deployable module is accomplished by means of 3D printing and soft lithography. The proposed strategy is to design and fabricate the whole soft deployable module through a one-stage molding process. The detail fabrication process is described as follows. Each soft module is fabricated by first building an ABS overall mold with through FDM with small holes for positioning of the SMA wire within the actuator structure. The connecting grooves between the two cavities for the two actuators of the overall mold will allow the formation of soft joints. The embedded reinforcement plate with slots for connecting the two stiff reinforcements is cut from a piece of polyvinyl chloride (PVC) plate with a thickness of 0.3 mm using a laser machine (M-300 laser platform, Universal Laser Systems). NIB magnets are positioned by the 3D printed stiff reinforcement, and then, the components are placed in the overall mold. The SMA wire is placed in the overall mold through its holes, pre-strained through mechanical loading, and held in place with the help of bolts attached to a fixture. The SMA wire is pre-strained with a fixed load of 1000 gram in order to obtain a stable working state with an approximate pre-strain of 5-6%. Third, PDMS is mixed with a base-to-catalyst ratio of 10:1, poured into the mold and cured for 8 h at 55°C, which is below the austenite transformation temperature of the SMA wires. After curing of the polymer, the soft module can be obtained after removing the overall mold.

Control unit. Through experimentation, the actuating currents for the 0.203 mm (0.008 in) diameter SMA wires embedded in the SSC were determined to be 0.90 A (in the air) and 0.95 A (in the water), respectively. A current control board connected to a CompactRIO 9024

embedded real-time controller and a NI 9264 module (National Instruments) is used to control the current applied to the SMA wires embedded in the modules, and Labview 2012 is used to input the current patterns. Using this experimental setup, the current patterns are set individually, including the actuation time and the magnitude of the currents for each channel.

Mechanical model for soft hinge actuators. In order to predict the bending deformation, a mechanical model by using Brinson modeling and Euler beam theory was developed and applied to the proposed soft hinge actuators composed of the soft deployable modules. The actuators are composed of pure bending segments whose deformed shape can be approximately regarded as circular arc. The schematic of the bending deformation is described as followed.

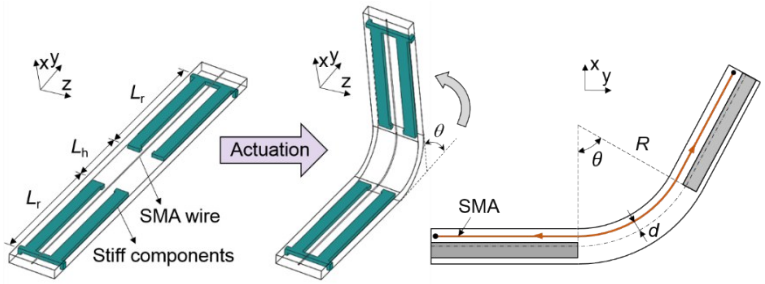

Figure S1. Schematic of the soft hinge actuator before actuation and during actuation.

The first step in the model is to express the stress and the strain of the SMA wires as a function of the bending angle of the actuator. First, the longitudinal stress ($\sigma_{\mathrm{L,act}}$) in the hinge actuator can be expressed as a function of the force generated by sum of all SMA wires as follows:

$$\sigma_{\mathrm{L,act}} = \frac{F_{\mathrm{SMA}}}{A_{\mathrm{act}}} \tag{1}$$

where F_{SMA} is the force generated by SMA wires and A_{act} is the area of the cross-section of the actuator. The longitudinal strain of the actuator is then expressed in terms of the longitudinal deformation of the actuator (ΔL) and of F_{SMA} , and the bending deformation of the actuator (θ) as a function of M and the flexible length of the actuator (L_{f}):

$$\varepsilon_{\mathrm{L,act}} = \frac{\Delta L}{L} = \frac{\sigma_{\mathrm{L,act}}}{E_{\mathrm{act}}} \tag{2}$$

$$R\theta - (R-d)\theta = \theta d = (\varepsilon_0 - \varepsilon_{\mathrm{cur}} - \varepsilon_{\mathrm{L,act}})L_{\mathrm{act}} \tag{3}$$

$$\frac{\theta}{L_{\mathrm{f}}} = \frac{M}{E_{\mathrm{act}} I} = \frac{F_{\mathrm{SMA}} d}{E_{\mathrm{act}} I} \tag{4}$$

where ε_0 and ε_{cur} are the initial strain and current strain of the SMA wire, d is the distance between the SMA wires and the middle place of the actuator structure, E_{act} is the Young's Modules of the actuator and I is the moment of inertia of the cross-section of the actuator structure, L_{act} is the total length of the embedded SMA wire. The stress in the SMA wire (σ_{SMA}) in terms of F_{SMA} is calculated as follows:

$$F_{SMA} = n_{SMA}\sigma_{SMA}A_{SMA} \tag{5}$$

where n_{SMA} is the number of the SMA wires embedded in the matrix and A_{SMA} is the cross-sectional area of each SMA wire.

The stress that the SMA wires are capable of producing depending on the strain is calculated using an SMA constitutive model, which describe the relationship between the stress, strain, temperature and the crystallographic phase of the material. In this research, the one-dimensional Brinson model is used to model the behavior of the SMA wire:

$$\sigma\text{-}\sigma_0 = E(\varepsilon\text{-}\varepsilon_0) + \Omega(\xi\text{-}\xi_0) + \Theta(T\text{-}T_0) \tag{6}$$

where σ and σ_0 are the current and initial stresses, $E = \xi E_m + (1-\xi)E_a$ is the Young's modulus of the SMA materials, ε and ε_0 are the current and initial strains, $\Omega = -E\varepsilon_L$ is the phase transformation contribution and ε_L is the maximum recoverable strain, ξ and ξ_0 are the current and initial martensite fractions, Θ is the thermal expansion factor, and T and T_0 are the current and initial temperatures. Assuming the initial stress to be zero, a negligible thermoelastic term and an initially fully martensite phase, we obtain:

$$\varepsilon = \frac{\sigma}{E} + \varepsilon_L(\xi - 1) + \varepsilon_0 \tag{7}$$

when the initial strain of the SMA wire is assumed to be equal to the maximum recoverable strain, equation (7) can be rewritten in:

$$\varepsilon = \frac{\sigma}{E} + \varepsilon_L\xi \tag{8}$$

During the strain recovery of the SMA wire for the martensite to austenite phase transformation, its martensite fraction can be calculated as follows:

$$\xi = \frac{\xi_0}{2}\left\{\cos\left[a_A(T - A_s) - \frac{a_A\sigma}{C_A}\right] + 1\right\} \tag{9}$$

for $C_A(T-A_f)<\sigma<C_A(T-A_s)$ when $T>A_s$. $a_A=\pi/(A_f-A_s)$ is a curve-fitting parameter, T is the wire's temperature assumed to be constant as 100°C experimentally during the whole process of strain recovery. C_A is a curve-fitting parameter to be equal to 10.3 according the previous studies. Finally, the stress from the SMA can be calculated using (8) and (9).

Table S1. Material properties of SMA (Flexinol).

Parameter	Value
Martensitic Young's modulus	E_{Mar}=28 GPa
Austenitic Young's modulus	E_{Aus}=75 GPa
Martensitic start temperature	M_S=52 °C
martensitic finish temperature	M_f=42 °C
Austenite start temperature	A_s=68 °C
Austenite finish temperature	A_f=78 °C
Wire diameter	152.4 um
Resistance per meter	55 Ω
Initial strain	ε_0=5%

Table S2. Main properties of PDMS (Sylgard 184).

Parameter	Value
Useful temperature range	-45 to 200 °C
Specific gravity	1.03 @ 25 °C
Heat cure	8 hours @ 58 °C
PDMS Young modulus	E_{PDMS}=1.8 MPa (25 °C)
Thermal conductivity	0.27 W/m K
Volume Resistivity	2.9×10^{14} Ω-cm

Performance of soft hinge actuators. Experiments were conducted to understand the effect of different design parameters on the bending performance of the actuator. To do so, the dimension of the cross section of all actuators was fixed at 15 × 3 mm (width × thickness) and the distance between the SMA wire and the neutral plane of the actuator was fixed at 1 mm during the fabrication process. A thermal camera (CX-320U, Hanmac) at ambient temperature (27°C) is used to detect the temperature change of the positions of SMA (point T) in real-time and the results are shown in Figure S2a. A thermal camera at ambient temperature (27°C) was used to measure the temperature change of the positions of SMA (point T) in real-time during the deploying process, and the results are shown in Figure S2a. From the results, it can be seen that the temperature of the SMA increases rapidly (curve AB) and that it takes around 20 s for the hinge actuator to achieve the maximum bending deformation. Also, the highest temperature with an applied electric current of 0.9 A is around 100 °C which is also used for modeling of the soft hinge actuators.

In the first experiment, the effect of the length of the rigid segment of the actuator on the bending capability is analyzed by keeping constant the length of the flexible segment at 20 mm and by varying the length of the rigid segments. Three samples were fabricated for each configuration with total rigid segment lengths ranging from 0 mm to 160 mm in increments of 20 mm. The results are shown in Figure S2b for the maximum bending curvature with fixed applied electric current of 1.0 A. It can be seen that the bending curvature goes up along with an increase in the length of the rigid segments. The second experiment is conducted with the length of the rigid segment being kept constant and by varying the length of the flexible segment. The length of each rigid segment is fixed at 40 mm with a total length of 80 mm for the rigid segments. Three samples were built for each actuator with a flexible segment length ranging from 10 mm to 70 mm in increments of 10 mm. The results are shown in Figure S2c for the maximum bending curvature. The results show that a longer flexible segment length leads to a smaller bending curvature, but larger bending angle.

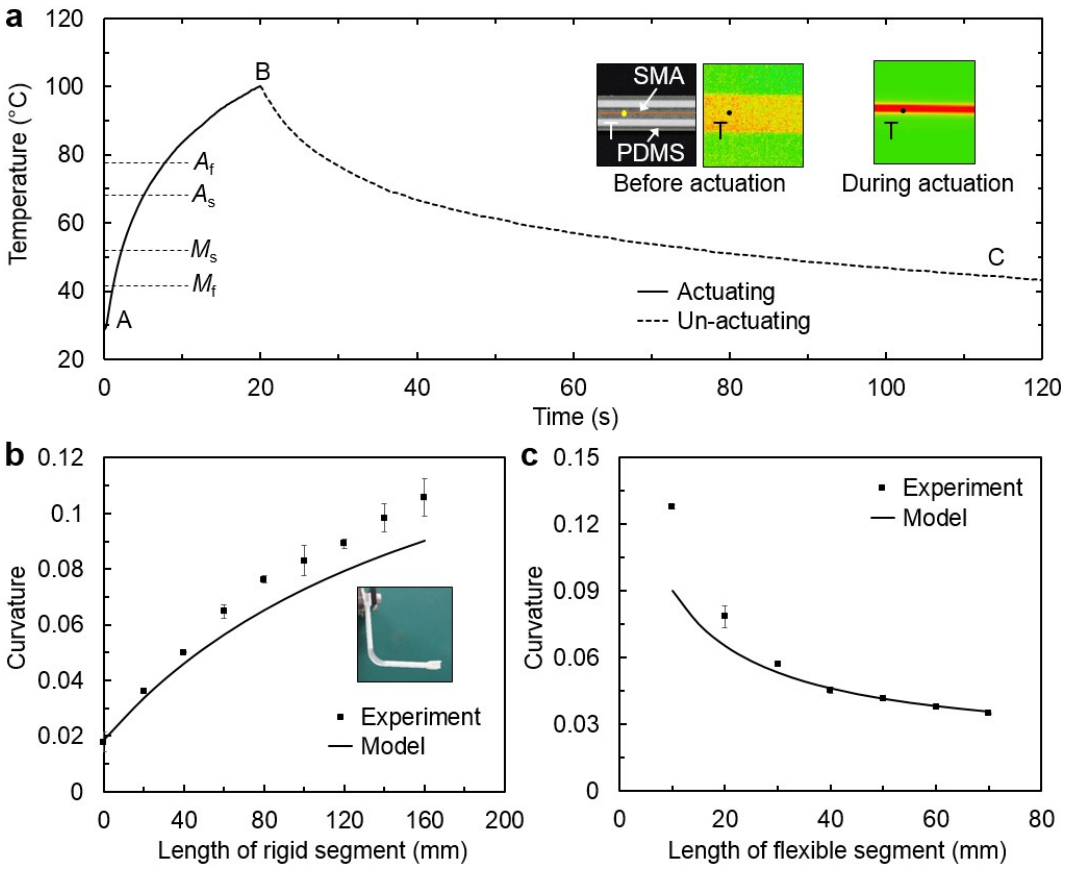

Figure S2. Performance of soft hinge actuators. (a) Temperature change of the SMA during actuation and after actuation. Insets show the visual temperature change of the surface of the actuator. Comparison of experimental and modeling results for hinge actuators with same length of flexible segment, but different length of rigid segment (b), and with same rigid segment length but different flexible segment length (c). Inset shows the configuration of one hinge actuator during actuation.

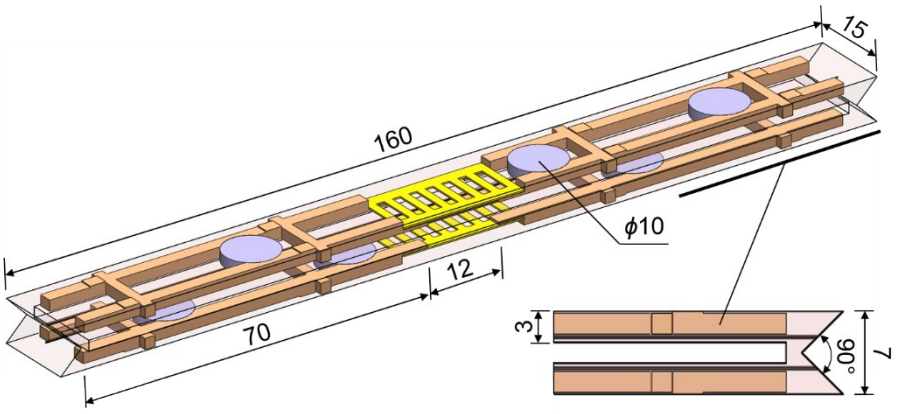

Figure S3. Configuration of soft deployable module before actuation and its important dimensions are drawn in the figure in the unit of millimeter.

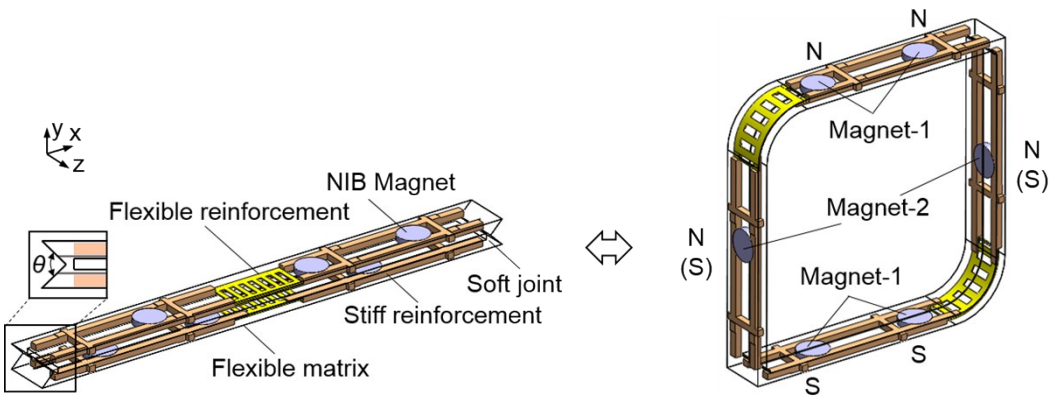

Figure S4. The magnets are placed at intervals in the block that minimizes unwanted interactions and each block contains 6 magnets with two pairs (named as magnet-1) being positioned on opposed segments, and one on (named as magnet-2) each of the other two segments. Magnet-1 with determined polarity direction is used for the connection between the soft blocks of the assembly. While magnet-2 is mainly used for locking the deployed quadrate deformation of a pair of adjacent soft modules, then there are two different designs that the polarity direction of magnet-2 where N-pole or S-pole points to the outside with the corresponding names of the fabricated modules of N-module and S-module. When an N-module and an S-module under locking state, their deployed quadrate configurations can be maintained even without continuous actuation.

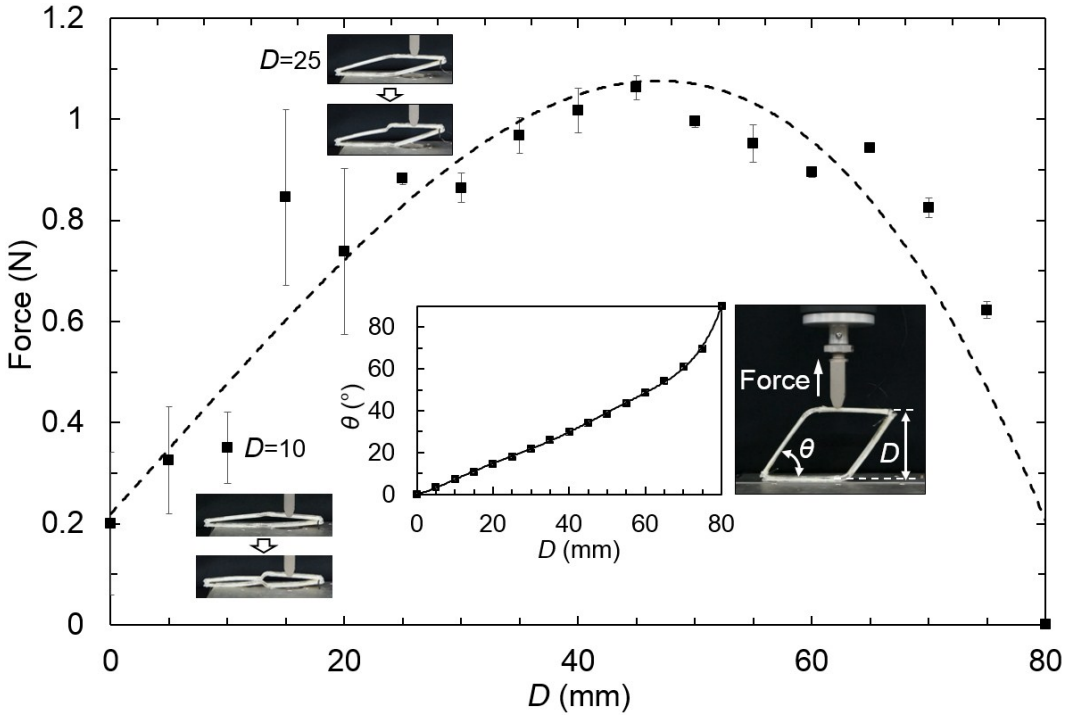

Figure S5. Deploying force of the soft module. The module is fixed flat on the ground and is then actuated. With a fixed distance D from the force measurement apparatus, the maximum upward deploying force is measured using the force-measurement instrument (Instron 5948). Results show that the module with a D equal to 45mm (θ is around 35°) has the highest upward deploying force. With D smaller than 40 mm (θ<35°), there is an obvious distortion of the flexible hinge section. With D larger than 45 mm (θ>35°), there is no such distortion of the flexible hinge section. Insets show the distorted configuration of the hinge section of the module when D is equal to 10 mm (around 7°) and 25 mm (around 18°). The smaller D is, the larger the distortion of the hinge. Other insets show the experimental setup and the relation between the deformation D and the deploying angle of θ.

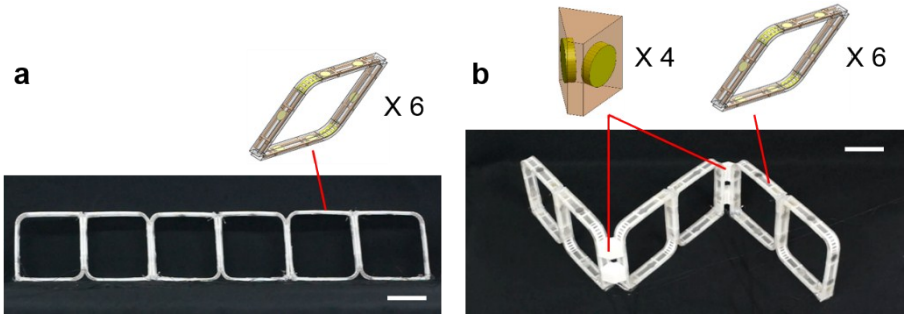

Figure S6. Components of the series-connected assemblies. (a) The deployed linear assembly and its components. (b) The deployed zigzag-shape assembly and its components where the included angle of the 3D printed wedge structure is 90°. The modules are either N-modules or S-modules. The schematics of the components are not in the same dimension scale. All scale bars are 50 mm.

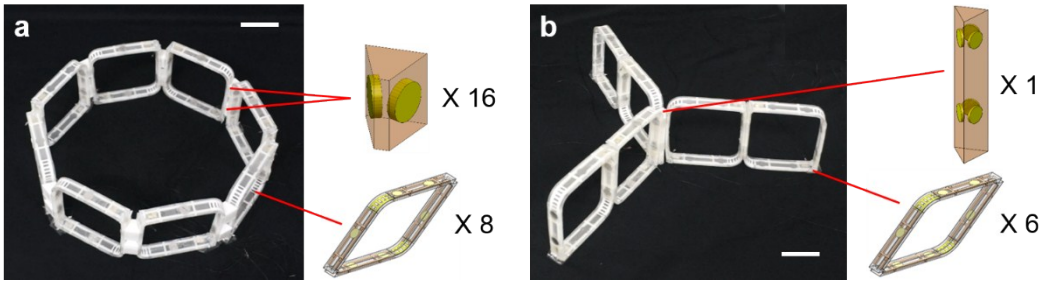

Figure S7. Components of the planar soft deployable assemblies. (a) The deployed eight-edge ring planar assembly and its components where the included angle of the 3D printed wedge structure is 45°. (b) The deployed radial-shape planar assembly and its components where the central hub has an equilateral triangle cross-section with the edge length is 15 mm. The modules are either N-modules or S-modules. The schematics of the components are not in the same dimension scale. All scale bars are 50 mm.

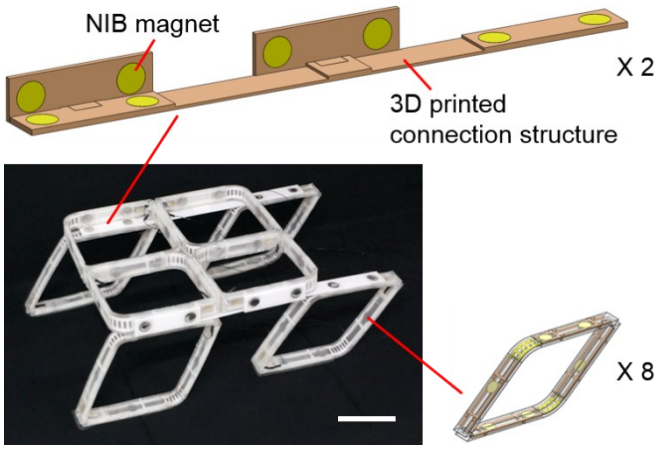

Figure S8. DeployBot and its components. The deployed configuration of the DeployBot where four modules are connected forming the body of the robot and four modules play the role of the four legs. The schematics of the components are not in the same dimension scale. All scale bars are 50 mm.

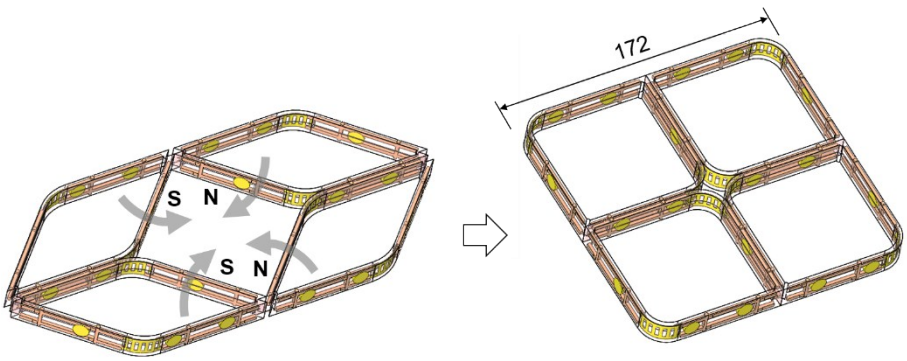

Figure S9. The deploying process of the body structure of DeployBot. The body structure are composed of four soft deployable modules (two N-modules and two S-modules) and its deployed configuration can be achieved and locked is in a field shape (by means of magnet-2). The important dimension is drawn in the figure in the unit of millimeter.

Supplementary movies

Movie S1. The deploying process of the soft deployable module.
Movie S2. The locking process of a pair of soft deployable modules.
Movie S3. DeployBot: fast assembling, deploying, and walking.